# Characterizing equilibrium in epitaxial growth

P. N. Patrone[1,2], R. E. Caflisch[3], and D. Margetis[4]
[1] *Department of Physics, and Institute for Research in Electronics and Applied Physics, University of Maryland College Park - MD 20742, USA*
[2] *Center for Nanoscale Science and Technology, National Institute of Standards and Technology, Gaithersburg - MD 20899, USA*
[3] *Department of Mathematics, and Institute for Pure and Applied Mathematics, University of California, Los Angeles - CA 90095, USA and*
[4] *Department of Mathematics, and Institute for Physical Science and Technology, and Center for Scientific Computation and Mathematical Modeling, University of Maryland, College Park - MD 20742, USA*

Using a kinetic model of epitaxial growth, we describe how geometry controls kinetic pathways through which external deposition influences the state of a vicinal surface. The state of the surface is determined by three key, adjustable parameters: the local step angle $\theta$, Péclet number $P$, and single bond detachment rate $\breve{b}$. By scaling arguments in $P$, we find three steady state regimes. In one regime, detailed flux balance approximately holds, so that the system is near equilibrium. In the other two regimes, geometric effects compete with deposition as the system is driven progressively out of equilibrium. Our analytical results are in excellent agreement with those of kinetic Monte Carlo simulations.

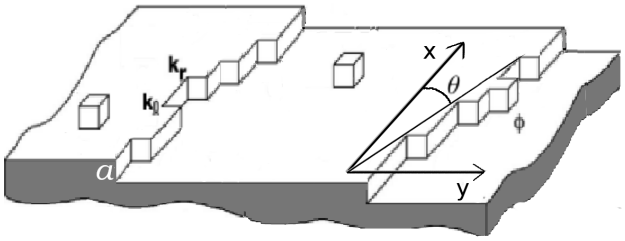


FIG. 1. Schematic of step geometry. The parameter $a$ is the atomic step height. The symbols $\phi$, $k_r$, and $k_l$ are the densities of edge adatoms, right facing, and left facing kinks, respectively. The local step angle is $\theta$.

Epitaxial growth involves a competition between certain atomistic processes that disrupt equilibrium and others that tend to restore it[1]. It is often unclear whether such *growth* phenomena can be understood in terms of *equilibrium* principles; nonetheless, concepts such as the free energy and local chemical potential are often invoked in descriptions of epitaxial systems[2–7].

Kinetic models that are valid in and out of equilibrium provide an alternate perspective of surfaces. This can yield insight into the conditions necessary for the use of thermodynamic concepts. For crystal surfaces, an important question (in the context of a kinetic model) is therefore: when is an epitaxial system close to equilibrium, and how can experimental parameters be used to control the state of the system? The rates of deposition and kinetic processes at step edges are usually seen as the key factors controlling growth[2–6]. Changing the *local* geometry at a step edge can also favor certain kinetic processes[3], so that the microstructure of a step should play a critical role in determining the state of the system.

Our goal in this Letter is to provide a criterion, in the context of a tractable model, that indicates when an epitaxial system is near equilibrium, as opposed to other *kinetic* steady states. We address two tasks. First, we define the state of the system by means of the kink density (number of atomic defects per unit length of a step). Second, we show how experimentally adjustable parameters, e.g. the local step angle $\theta$ and the Péclet number $P \propto F/D_e$, can control what state the system is in ($F$ is the external deposition rate, and $D_e$ is a diffusivity associated with atomic motion at a step). In particular, we show how increasing $\theta$ favors a return to equilibrium by creating additional kinks for adatoms to attach to.

Our work is motivated by the issue of how accurately experimental surface systems can be described by near-equilibrium theories based on the celebrated Burton-Cabrera-Frank (BCF) model[3–6]. By starting with a more general kinetic model, which contains information about kinks, we aim to provide some insight into the conditions necessary for the validity of BCF-type theories. A broader goal of our work is to describe qualitative features of surfaces under high growth conditions.

Our description of surface kinetics, particularly near-equilibrium kinetics, differs from works based on the fluctuation-dissipation theorem, e.g. ref.[8]. Here, we use the density of point defects (kinks), as opposed to correlations between positions of defects[8], to determine when the system is near equilibrium.

We adopt a modified version of the mean field, step-edge model in[9,10], which describes surfaces in and out of equilibrium (see also[11] for related works). Features of our model are depicted in fig. 1, which shows two steps separated by a terrace on a typical crystal surface[2,3]. The steps have atomic height $a$, and atoms are deposited on the surface at rate $F$. Adsorbed atoms (adatoms) diffuse on terraces, and may attach to and detach from step edges[3]. For our present purposes, it suffices to study the {001} face of a single step on a simple cubic lattice. At a step edge, we distinguish between edge, kink, and boundary adatoms, which have one, two and three nearest in-plane neighbors, respectively. The densities of edge and kink adatoms are $\phi$ and $k$. Kinks can be right or left facing, with densities $k_r$ and $k_l$ (cf. fig. 1).

Morphological changes to the surface occur via step motion, which in turn results from atomistic processes that create and destroy kinks[2]. Specifically, to advance a step locally, an edge adatom must either (i) attach to an existing kink, (ii) form a left-right kink pair by attaching to another edge adatom, or (iii) annihilate a right-left kink pair (cf. fig. 2)[9,10]. The reverse processes cause steps to retreat.

We identify equilibrium as the state in which *detailed flux balance* (DFB) holds for all atomistic processes causing step motion[12,13]. By detailed flux balance, we mean that the net rate of any process (the product of a single particle transition rate and the density of atoms eligible to make that transition) equals the net rate of its reverse process[9].[?] The kink density plays a *central* role in determining when the system is near equilibrium, since $k$ connects kinetic processes to the local step geometry.

Therefore, we begin our analysis by writing

$$k_r + k_l = k, \qquad k_r - k_l = a^{-1} \tan\theta, \tag{1}$$

Assuming that steps have a well defined direction, we take $\theta$ to be spatially constant along the step edge. We also

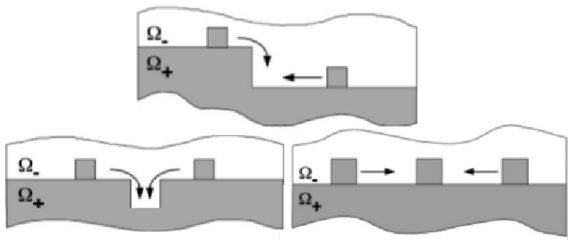


FIG. 2. Top down view of the processes by which a step moves locally. The symbols $\Omega_+$ and $\Omega_-$ denote the upper and lower terraces at a step edge, respectively. Starting from the top and going clockwise, the coordination numbers for these processes are $c_1 = c_2 = c_3 = 2$; cf. eqs. (2) and (3).

take the edge adatom ($\phi$) and kink ($k$) densities to be spatially constant, so that they obey

$$\partial_t \phi = FL + c_1(a^{-2} D_k k - a^{-1} D_e \phi k), \tag{2}$$

$$\partial_t k = \frac{2c_2}{a}(D_e \phi^2 - D_k k_r k_l) + \frac{2c_3}{a^3}(D_b - a^3 D_e \phi k_r k_l), \tag{3}$$

where $L$ is the average terrace width, and $D_e$, $D_k$, and $D_b$ are the diffusivities of edge, kink, and boundary adatoms[9,10]. The constants $c_1$, $c_2$, and $c_3$ are coordination numbers measuring the number of pathways by which edge adatoms and kinks can be created or destroyed (cf. fig. 2). The factors of 2 appearing in eq. (3) account for the fact that the corresponding processes create and destroy kink *pairs*.

Equations (2) and (3) are simplified versions of the evolution equations given in[9,10]. The right-hand side of eq. (2) states that (i) all deposited adatoms move to a step edge (via the term $FL$), (ii) atoms detach from kink sites with probability $k$ at a rate $D_k$, and (iii) edge adatoms attach to kink sites with probability $\phi k$ at a rate $D_e$. The term $c_1$ in eq. (2) indicates that the processes of adatom detachment-attachment at a kink site occur by $c_1$ different pathways. Equation (3) and the coefficients $c_2$ and $c_3$ can be interpreted similarly (cf. fig. 2).

The parent model in[9,10] (from which eqs. (2) and (3) are taken) also includes an evolution equation for the density $\rho$ of adatoms on a terrace. Consequently that model contains terms proportional $\rho k$ and $\rho\phi$ describing processes in which terrace adatoms attach directly to kinks or edge adatoms (as opposed to a straight step edge). Here we assume that *products* of densities involving $\rho$ are negligible. This approximation is realized in eq. (2) via the source term $FL$; all terrace adatoms become edge adatoms. Equations (2) and (3) also disregard detachment of atoms from a step, so that we only allow for diffusion *along* a step edge.

We assume that the diffusion coefficients[?] are

$$D_\ell = D_T \exp(-E_\ell / k_B T), \tag{4}$$

where $D_T$ is the diffusion coefficient for adatoms on a terrace, $\ell = e, k$, or $b$ for edge, kink, or boundary adatoms, and $E_\ell = n_\ell E_{\rm bond}$; $E_{\rm bond}$ is the energy of a single atomic bond, and $n_\ell$ is the number of nearest in-plane neighbors of a given adatom type[2,9]. Note that $n_\ell = 1, 2$ or 3 for $\ell = e, k$, or $b$. We also define the single bond detachment rate $\breve{b} = D_k/D_e = D_b/D_k = \exp(-E_{\rm bond}/k_B T)$.

We look for steady states by setting the time derivatives equal to zero in eqs. (2) and (3), so that

$$P = c_1(a^2 \phi k - a\breve{b} k), \tag{5}$$

$$c_2 a^2(\breve{b} k_r k_l - \phi^2) = c_3(\breve{b}^2 - a^3 \phi k_r k_l). \tag{6}$$

The parameter $P = aLF/(D_e/a^2)$ represents a competition between two atomistic processes; the numerator, $aLF$, is the flux of deposited adatoms arriving at a step edge, which drives the system *out of equilibrium*, since it violates DFB. The denominator, $D_e/a^2$, is the rate at which edge adatoms diffuse (i.e., hop) along a step edge. This diffusion is the fastest process by which the system may re-equilibrate. Hence, $P$ should help control how close the system is to equilibrium. In this study we assume that $P \ll 1$ and $\breve{b} \ll 1$, which corresponds to a regime in which the adatom density $\phi$ is low.

We begin by considering the case $F = 0$ (i.e., $P = 0$), so that eqs. (5) and (6) imply $\phi = \breve{b}/a$ and $k_r k_l = \breve{b}/a^2$. Then, by eq. (1),

$$k = a^{-1}(\tan^2\theta + 4\breve{b})^{1/2}. \tag{7}$$

This is an equilibrium solution, since it satisfies DFB; i.e., $D_k k = a D_e \phi k$, $D_e \phi^2 = D_k k_r k_l$, and $D_b = a^3 D_e \phi k_r k_l$ (cf. eqs. (2) and (3)).

In eq. (7), the terms in parentheses reveal two distinct sources of kinks. The term $a^{-2}\tan^2\theta = (k_r - k_l)^2$ corresponds to *geometric* (forced) kinks; these arise solely from the non-zero step angle and all face the same direction (for example, if $\theta > 0$, then $k_r > k_l$, and geometric kinks are right facing). The term $4\breve{b}$ is associated with *thermal* kinks, which are created when adatoms detach from kinks or edges and attach to each other. Thermal kinks always come in left-right pairs and do not contribute to the average step angle. When the single bond energy becomes large ($\breve{b} \to 0$), detachment processes rarely occur, and the equilibrium kink density is given by the geometric kink density ($k \to |\tan\theta|/a$).

For nonzero $P$, it is convenient to rescale variables, letting $l = ak/\breve{b}^{1/2}$, $q = P/\breve{b}^{3/2}$, and $\psi = \tan(\theta)/\breve{b}^{1/2}$. Algebraic manipulations of eqs. (5) and (6) then yield

$$c_1^2\left[c_3 + c_2\right] l^4 + c_1 c_3 q l^3 - c_1^2\left[c_3 + c_2\right](4 + \psi^2) l^2 \\ -c_1\left[c_3\psi^2 + 8c_2\right] ql - 4c_2 q^2 = 0. \tag{8}$$

This fourth-order algebraic equation for $l$ (i.e., for $k$) can be solved exactly, but we resort to approximations that are more useful for physical interpretation. There are three distinct regimes in which the solution to eq. (8) may be simplified: (i) $q \ll (1+\psi^2)^{1/2}$; (ii) $(1+\psi^2)^{1/2} \ll q \ll (1+\psi^2)^{3/2}$; and (iii) $(1+\psi^2)^{3/2} \ll q$. Note that regime (ii) only exists if $1 \ll |\psi|$, so that it could be rewritten as (ii') $|\psi| \ll q \ll |\psi|^3$. The kink density $k$ solving eq. (8) is found approximately in these three regimes to be

$$k \approx a^{-1}(\tan^2\theta + 4\breve{b})^{1/2}, \qquad P \ll \breve{b}(\breve{b} + \tan^2\theta)^{1/2} \tag{9}$$

$$k \approx a^{-1}|\tan\theta|, \qquad \breve{b}|\tan\theta| \ll P \ll |\tan\theta|^3 \tag{10}$$

$$k \approx a^{-1}[4c_2 P/(c_1 c_3)]^{1/3}, \qquad (\breve{b} + \tan^2\theta)^{3/2} \ll P. \tag{11}$$

In eq. (9), the kink density is approximately equal to the value given by eq. (7); corrections to eq. (9) are of size $P$. We call this the "*near-equilibrium*" (NE) regime, since DFB is approximately satisfied; indeed the dominant balance in eq. (5) is $a^2\phi k \approx a\breve{b}k \gg P$.

Equation (11) corresponds to a state in which information about the step angle $\theta$ is lost; the kink density is entirely determined by the Péclet number. Since the presence of $P$ in eq. (11) implies that deposition determines the kink density, we call this regime the "*flux dominated steady state*" (FDSS). Detailed flux balance is lost in this kinetic steady state. The flux to the edge is balanced by flux of edge adatoms to kinks. The creation of kink pairs from two edge adatoms is balanced by the hopping of an edge adatom to fill in a single missing atom in the edge (a kink pair), as illustrated in fig. 2; i.e., eqs. (5) and (6) imply

$$c_1 a^2 \phi k \approx P, \tag{12}$$

$$c_2 \phi^2 \approx c_3 a \phi k_r k_l. \tag{13}$$

In the intermediate regime governed by eq. (10), which we call the "*angle-dominated steady state*" (ADSS), kinks are predominantly geometric. For example, if $\theta > 0$, then $k_r \gg k_l$, so that $k_r \approx a^{-1}|\tan\theta|$. A higher-order correction yields $k_l \approx a^{-1}c_2 P/(c_1 c_3 \tan^2\theta)$. This correction term for the ADSS is determined by the dominant kinetic balances, eqs. (12) and (13) as in the FDSS.

Although the ADSS does not satisfy DFB, it may be interpreted as an extension of the NE regime: the ADSS amounts to an increase (relative to the NE regime) of the range of $\breve{b}$ and $P$ values for which the kink density is approximately independent of the deposition rate. As $\breve{b}$ decreases (keeping $P, \theta \neq 0$ fixed) in the NE regime, the system transitions *continuously* from NE to the ADSS (cf. fig. 3). If instead $P$ and $\breve{b}$ are held fixed, increasing $\theta$ can eliminate the flux dependence of $k$ (cf. fig. 4).

The ADSS kink density is controlled by the step angle alone (and not $P$ or $\breve{b}$) because *geometric* kinks inhibit the formation of left-right kink pairs. This can be seen by considering the length $\tilde{a} = a/\tan\theta$ and time $\tilde{t} = \tilde{a}^2/D_e$, which are the average length between geometric kinks and the average time for a single edge adatom to traverse the distance $\tilde{a}$. Rewriting the ADSS condition $P \ll |\tan^3\theta|$ (cf. eq. (10)) in the form $\tilde{t} \ll (\tilde{a}LF)^{-1}$ and noting that $1 \ll |\psi|$ is equivalent to $\tilde{t} \ll a^2/D_k \ll a^2/D_b$ suggests that an edge adatom attaches to an adjacent geometric kink long before another edge adatom is created within a distance $\tilde{a}$ by either deposition or detachment. Thus, in the ADSS, geometric kinks shield edge adatoms from each other, so that left-right pairs rarely form.

In order to test our analytical results, we performed kinetic Monte Carlo (kMC) simulations of a cubic, solid-on-solid surface model. Details of the algorithm may be found in[14,15]. The main idea is to move adatoms with probabilities proportional to their diffusion rates, given by eq. (4). We modeled the surface on a 500 $a$ × 200 $a$ rectangular grid, whose sides were parallel to the $x$ and $y$ axes of the crystal (cf. fig. 1). The surface was initialized to have four steps separated by terraces 50 atomic lengths wide. The $x$ axis corresponded to $\theta = 0$ (cf. fig. 1). Nonzero step angle was incorporated by applying screw periodic boundary conditions along lines making an angle $\theta$ with the $x$-axis; realizable values of $\theta$ for this simulation were those satisfying $\tan\theta = j/500$ for some integer $j$.

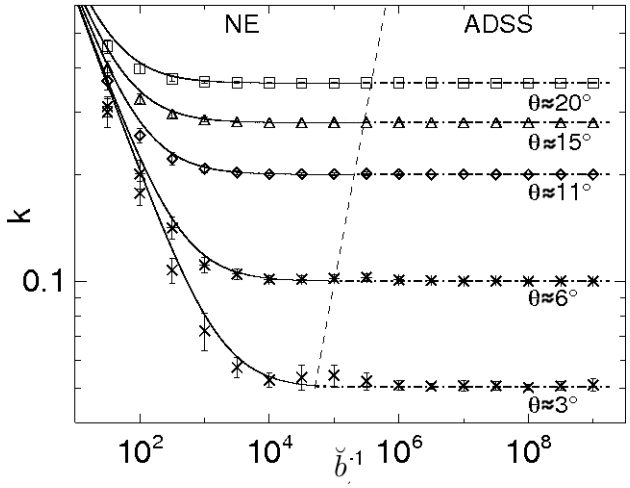


FIG. 3. KMC-simulated kink densities (symbols with error bars) versus eqs. (9) and (10) (solid and dash-dot lines, respectively). The slanted dashed line indicates the approximate boundary between the NE and ADSS regimes; it is the solution to $P = \breve{b}|\tan\theta|$. We fixed $P = 10^{-6}$ for these simulations. The ADSS kink density exhibits the same behavior as the NE kink density taken in the limit $\breve{b} \to 0$.

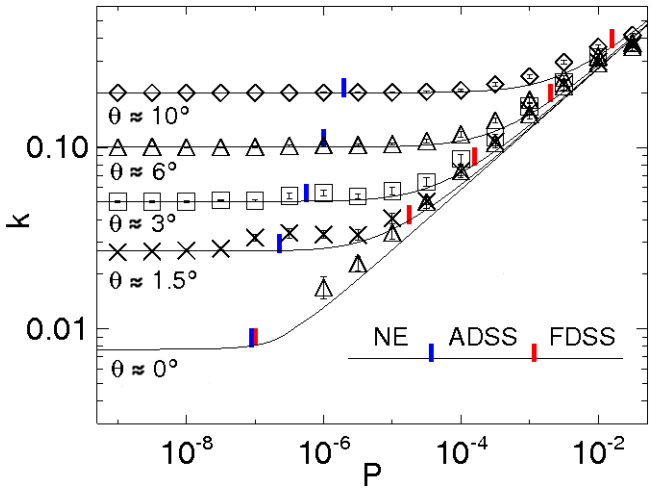


FIG. 4. [Color online] Analytic (solid lines) and kMC (symbols) kink densities as functions of $P$. Analytic densities were found by numerically solving eq. (8). The kink densities collapse to a single curve as $P$ increases. For each $\theta$, blue and red vertical lines indicate the locations of the NE to ADSS and ADSS to FDSS transitions, going left to right. We omit NE kMC data for $\theta = 0$; significantly larger simulations are required to suppress fluctuations in this data. We set $\breve{b} = 10^{-5}$ and disabled island nucleation in these simulations.

We compare simulated kink densities with the analytic predictions from eqs. (9)-(11), as a function of $\breve{b}$ in fig. 3 and as a function of $P$ in fig. 4. Both figures show excellent agreement between the model predictions and the results from kMC simulations in all three regimes. This is true even for kink densities $k$ of size up to 0.4, which is somewhat surprising, since we do not expect our mean-field model to be valid when any density becomes comparable to unity (i.e., adatom and kink correlations could significantly alter the form of eqs. (2) and (3)). Morever, fig. 3 confirms our conclusion that the ADSS exhibits NE behavior, since it shows that the NE kink density approaches the ADSS kink density as $\breve{b}$ becomes small. Also, fig. 4 confirms that the kink density is approximately independent of the step angle in the FDSS regime (i.e., to the right of the red bar on each curve).

Our model does not take into account island formation; this process will decrease the magnitude of $P$ (via $FL$), since not all of the deposited adatoms will diffuse to a step. More generally, we ignore the effects that terrace inhomogeneities such as islands and voids have on a step.

We believe that our analytical results, eqs. (9)–(11), are experimentally testable by means of molecular beam epitaxy (MBE) and *in situ* scanning-tunneling microscopy (STM). For example, certain STM designs permit atomic resolution imaging of Si(111) surfaces *during growth*[16,17]. Since diffusion rates are functions of temperature[2], and the deposition rate can be controlled during MBE, $P$ and $\breve{b}$ correspond to experimentally adjustable parameters.

Therefore, we expect that it should be possible to experimentally observe the active kinetic processes implied by the dominant balances in eqs. (5) and (6).

In conclusion, we presented a mean field model of epitaxial growth to demonstrate how varying the step angle $\theta$, deposition rate $F \propto P$, and single bond detachment rate $\breve{b}$, determines whether a vicinal surface is in equilibrium or in a non-equilibrium steady state. We showed that the system has three steady-state regimes. In one regime, the system obeys detailed flux balance and is near equilibrium. In the other two regimes, the behavior of the system is determined by $\theta$ and $P$, respectively. Our analysis is in excellent agreement with kMC simulations in all three regimes. We hope that our characterization of active kinetic processes in surface systems can be further explored by STM measurements during growth.

*Acknowledgements* The first author (PNP) acknowledges support under the National Institute of Standards and Technology American Recovery and Reinvestment Act Measurement Science and Engineering Fellowship Program Award No. 70NANB10H026 through the University of Maryland; and by NSF MRSEC Grant No. DMR 0520471 at the University of Maryland. The second author (REC) was partially supported by NSF Grant No. EFRI 1025104. The third author (DM) was supported by NSF Grant No. DMS 0847587. The authors wish to thank T L Einstein and R Sharma for helpful comments during preparation of the manuscript.

[1] Evans J. W., Thiel P. A., Bartelt M. C., Surf. Sci. Rep. **61** (2006) 1.
[2] Jeong H. -C. Williams E. D., Surf. Sci. Rep. **34** (1999) 171.
[3] Burton W. K., Cabrera, N., Frank F. C., Phil. Trans. R. Soc. London A **243** (1951) 299.
[4] Pierre-Louis O. Misbah C., Phys. Rev. B **58** (1998) 2259.
[5] Ghez R., Cohen H., Keller J., J. Appl. Phys. **73** (1993) 3685.
[6] Liu F. Metiu H., Phys. Rev. E **49** (1994) 2601.
[7] Pimpinelli A. Villain J., Physics of Crystal Growth, Cambridge U. Press, Cambridge, 1998.
[8] Kallunki J. Krug J. Surf. Sci. Lett. **523** (2003) L53.
[9] Caflisch R. E., E W., Gyure M. F., Merriman B., Ratsch C., Phys. Rev. E. **59** (1999) 6879.
[10] Margetis D. Caflisch R. E., Multiscale Model. Simul. **7** (2008) 242.
[11] Balykov L. Voigt A., Phys. Rev. E **72** (2005) 022601; Multiscale Model. Simul. **5** (2006) 45; Caflisch R. E. Li B., Multiscale Model. Simul. **1** (2003) 150; Filimonov S. N. Hervieu Yu. Yu., Surf. Sci. **553** (2004) 133.
[12] Gouyet J. -F., Plapp M., Dieterich W., Maass P., Adv. Phys. **52** (2003) 523.
[13] Zia R. K. P. Schmittmann B., J. Stat. Mech. (2007) P07012.
[14] Amar J. G. Comput. Sci. Eng. **8** (2006) 9.
[15] Voter A. F., Radiation Effects in Solids, NATO Science Series, Sickafus K. E., Kotomin E. A., Uberuaga B. P., Springer, Dordrecht (2007).
[16] Voigtländer B. Zinner A., Appl. Phys. Lett. **63** (1993) 3055; Voigtländer B., Zinner A., Weber Th., Rev. Sci. Instrum. **67** (1996) 2568.
[17] , Voigtländer B., Kästner M., and Šmilauer P., Phys. Rev. Lett. **81** (1998) 858.